



Moisture sorption characteristics of probiotic-fermented sea tangle powder and its thermodynamic properties

Daeung Yu¹ | Gicheol Kwon² | Moojoong Kim¹ | Young-Mog Kim³ | Soo-Im Choi⁴ | Gun-Hee Kim⁵ | **Donghwa Chung^{1,2,6}**

¹Institute of Food Industrialization, Institutes of Green Bio Science and Technology, Seoul National University, Pyeongchang, Republic of Korea

²Food Technology Major, Graduate School of International Agricultural Technology, Seoul National University, Pyeongchang, Republic of Korea

³Department of Food Science and Technology, Pukyong National University, Busan, Republic of Korea

⁴Plant Resources Research Institute, Duksung Women's University, Seoul, Republic of Korea

⁵Department of Food and Nutrition, Duksung Women's University, Seoul, Republic of Korea

⁶Center for Food and Bioconvergence, Seoul National University, Seoul, Republic of Korea

Correspondence

Donghwa Chung, Food Technology Major, Graduate School of International Agricultural Technology, Seoul National University, Pyeongchang 25354, Republic of Korea.

Email: dchung@snu.ac.kr

Funding information

Ministry of Oceans and Fisheries

Abstract

The moisture sorption characteristics of *Lactobacillus brevis*-fermented sea tangle powder were investigated. Moisture sorption isotherms were prepared at 4, 25, and 37°C in a water activity (a_w) range of 0–0.96 and exhibited typical J-shaped type III sorption characteristics, most likely due to the high carbohydrate content (65.7%) of the powder. The fermented sea tangle powder had greater moisture sorption capacity than those reported for other seaweeds, and changed to rubbery or liquid states when stored at $a_w > 0.5$. The Peleg and GAB models accurately described the sorption isotherms, and the monolayer moisture contents were 0.176–0.443 g water/g dry matter. The moisture sorption was an exothermic, enthalpy-driven, spontaneous process, and the enthalpy–entropy compensation existed with an isokinetic temperature of 448.1 K. The net isosteric heat of moisture sorption exponentially decreased from 15.02 to 0.49 kJ/mol as the equilibrium moisture content increased from 0.02 to 1.29 g water/g dry matter.

Practical applications

Sea tangle is known to possess various biological and nutraceutical properties, such as antitumor and anticoagulant, antiproliferative, and antioxidant activities, which is commercially available in Pacific and Asian countries as a traditional functional food. The present study investigating information of moisture sorption characteristics of *L. brevis*-fermented sea tangle powder will be useful to understand its strongly hygroscopic nature and resulting low storage stability, which limits the easy and convenience of its handling and application. The information also will be important for improving its shelf life and retaining quality across postharvest processing.

1 | INTRODUCTION

Sea tangle (*Saccharina japonica*) is an edible brown alga that belongs to the class Phaeophyceae and is regarded as a good source of health-promoting substances, such as dietary fiber, protein, carotenoids, vitamins, essential fatty acids, and minerals (Lee et al., 2010). It has been consumed as a traditional functional food, especially by pregnant women and children, since ancient times in Pacific and Asian countries, including Korea, Japan, and China

(Kang et al., 2012). Sea tangle is known to possess various biological and nutraceutical properties, such as antitumor and anticoagulant (Haroun-Bouhedja, Ellouali, Sinquin, & Boisson-Vidal, 2000), antiproliferative (Yuan & Walsh, 2006), and antioxidant activities (Wang, Zhang, Zhang, & Li, 2008). Sulfated polysaccharides, such as fucoidans, are recognized as the major active compounds in sea tangle. The alga also contains γ -aminobutyric acid (GABA), a non-protein amino acid that acts as a major inhibitory neurotransmitter and is known to have beneficial physiological properties, such as

hypotensive, diuretic, and tranquilizing activities (Lee et al., 2010). Lee et al. (2010) reported that the amount of GABA in sea tangle increased approximately 100 times when the alga was fermented with a probiotic bacterium, *Lactobacillus brevis*. Sea tangle fermented with *L. brevis* is now commercially available as a spray- or freeze-dried powder (Marine Bioprocess, 2018). However, its strong hygroscopic nature, and the resulting low stability during processing, handling, and storage, greatly limit use of the powder for the development of functional food products. Therefore, it is essential to improve understanding of the moisture sorption characteristics of the powder, to promote and broaden its applications.

The moisture sorption characteristics of several algae have been reported, including those of brown algae, such as *Fucus vesiculosus* (Moreira, Chenlo, Sineiro, Arufe, & Sexto, 2016) and *Bifurcaria bifurcate* (Moreira, Chenlo, Sineiro, Sánchez, & Arufe, 2016), and red algae, such as *Kappaphycus alvarezii* (Senthil, Mamatha, Vishwanath, Bhat, & Ravishankar, 2011), *Gracilaria* (Lemus et al., 2008), and *Gelidium sesquipedale* (Mohamed et al., 2005). Only *K. alvarezii* was prepared as a powder for the analysis of its sorption characteristics; the other algae that were studied were analyzed in their raw form or in small pieces. Most of the algae demonstrated J-shaped type III moisture sorption isotherms between approximately 5 and 65°C; however, *F. vesiculosus* demonstrated either a type III isotherm or a sigmoid-shaped type II isotherm, depending on the temperature (Moreira, Chenlo, Sineiro, Arufe, et al., 2016). In general, the algae were found to have an equilibrium moisture content (X_{eq}) of about 0.1–0.2 g water/g dry matter at water activity (a_w) below about 0.6–0.7, and exhibited sudden increases in X_{eq} up to about 0.65–1.20 g water/g dry matter when the a_w was increased to about 0.9. Halsey, Guggenheim–Anderson–de Boer (GAB), and modified Brunauer–Emmett–Teller (BET) models have been successfully used to describe the moisture sorption isotherms of the algae. The net isosteric heat of sorption of water (q_{st}) values measured for *F. vesiculosus*, *B. bifurcate*, and *G. sesquipedale* revealed a trend toward an exponential decrease as the X_{eq} increased (Mohamed et al., 2005; Moreira, Chenlo, Sineiro, Arufe, et al., 2016; Moreira, Chenlo, Sineiro, Sánchez, et al., 2016). Thermodynamic analyses revealed that moisture sorption was an enthalpy-driven process for *F. vesiculosus* and *B. bifurcate* (Moreira, Chenlo, Sineiro, Arufe, et al., 2016; Moreira, Chenlo, Sineiro, Sánchez, et al., 2016).

The objectives of this study were to (a) experimentally determine the moisture sorption isotherms of *L. brevis*-fermented sea tangle powder at 4, 25, and 37°C and an a_w of 0–0.96 to understand its high moisture susceptible nature, which limits the easy and convenience of its handling and application; (b) mathematically interpret the sorption isotherms using several empirical and semiempirical models, to understand the sorption mechanism and predict X_{eq} at a given a_w and temperature (where X_{eq} is a key parameter determining the storage conditions for applications of the powder); and (c) determine the net isosteric heat (q_{st}), entropy (ΔS), Gibbs free energy (ΔG), and isokinetic temperature (T_i) of the moisture sorption to characterize the thermodynamic nature of the moisture sorption of the fermented sea tangle powder.

2 | MATERIALS AND METHODS

2.1 | Materials

Fresh sea tangle (*S. japonica*) was purchased from Food & Food Co., Ltd. (Busan, Korea). Sea tangle powder fermented with *L. brevis* was supplied by Marine Bioprocess Co., Ltd. (Busan, Korea). Phosphorus pentoxide (P_4O_{10}), lithium chloride (LiCl), potassium acetate (CH_3COOK), magnesium chloride ($MgCl_2$), potassium carbonate (K_2CO_3), magnesium nitrate ($Mg(NO_3)_2$), potassium iodide (KI), ammonium sulfate ($(NH_4)_2SO_4$), and potassium nitrate (KNO_3) were purchased from Samchun Pure Chemical Co. Ltd. (Seoul, Korea).

2.2 | Preparation of sea tangle powder

L. brevis-fermented sea tangle powder was prepared according to the method of Kang, Qian, Lee, and Kim (2011). Briefly, sea tangle was rinsed with fresh water to eliminate foreign materials, and then soaked in twice the volume of water for 1 hr for desalinization. Desalinized sea tangle was dried at 60°C for 24 hr in a drying oven, and then ground using a grinder mill to prepare powder. The sea tangle powder was added to water at a ratio of 1:15 (w/v) with 3% (w/w) rice flour to aid in fermentation. Next, the mixture was autoclaved at 121°C for 30 min. *L. brevis* BJ20 (KCTC 11377BP) was cultured in de Man–Rogosa–Sharpe (MRS) broth at 37°C for 24 hr. The culture was used to inoculate the sea tangle solution at a concentration of 2% (v/v), and the inoculated solution was incubated at 37°C for 24 hr. Fermented sea tangle solution was filtered (0.1 μm filter) and freeze-dried (FD-550; Tokyo Rikakikai Co., Ltd., Tokyo, Japan) at –20°C for 48 hr with a vacuum pressure less than 5 Pa. The freeze-dried, fermented sea tangle powder was finely ground using a blender and stored at –4°C until further use.

2.3 | Proximate analysis

Proximate compositions of sea tangle powders before and after fermentation were analyzed. Moisture content was estimated by drying at 105°C for 4 hr (AOAC method 934.06, 2000). Protein content was determined using the Kjeldahl method with a conversion factor of 6.25 (AOAC method 979.09, 2000). Lipid content was analyzed using the gravimetric Soxhlet method (overnight extraction after oven drying at 80°C) (AOAC 960.39, 2000). Ash content was measured by heating the samples overnight in a muffle furnace at 550°C (AOAC method 923.03, 2000). Carbohydrate content was determined by calculating the difference from 100%. Salinity content was determined using Mohr's method with silver nitrate titration (Keup & Bayless, 1964). All analyses were performed in triplicate.

2.4 | Particle size measurement

The particle size of sea tangle powders before and after fermentation was determined using a laser diffraction particle size analyzer (Cilas 1190; Cilas, Orléans, France) and expressed in μm as

volume-weighted mean diameter ($d_{4,3}$), which was calculated using the following equation:

$$d_{4,3} = \frac{\sum n_i d_i^4}{\sum n_i d_i^3} \quad (1)$$

where n_i is the number of particles of class i and d_i is the diameter of class i . The span value, which is a polydispersity index of particle size distribution, was also calculated for the sea tangle powders using the following equation:

$$\text{Span} = \frac{d_{90} - d_{10}}{d_{50}} \quad (2)$$

where d_{10} , d_{50} , and d_{90} are the diameters of the powders at 10%, 50%, and 90% cumulative volume in particle size distribution, respectively. The $d_{4,3}$ and span values were calculated using SizeExpert software (ver. 9.51; Cilas).

2.5 | Determination of moisture sorption isotherms

Moisture sorption isotherms of the fermented sea tangle powder were determined by the gravimetric method at 4, 25, and 37°C. Nine saturated salt solutions were separately prepared by dissolving sufficient amounts of salt in deionized water, placed in glass desiccators, and equilibrated in a temperature-controlled chamber (HB-103LP; Hanbaek Scientific Co., Bucheon, Korea) at 4, 25, or 37°C for at least 24 hr to obtain a range of a_w from zero to about 0.92–0.96, depending on temperature (Table 1). The powder samples (2 ± 0.001 g) were evenly spread on pre-weighed aluminum dishes and placed in the equilibrated desiccators. Thymol (30 g in a 50 ml beaker) was placed inside the high a_w (>0.67) desiccators to prevent microbial growth. The desiccators were placed in the temperature-controlled chamber at 4, 25, or 37°C. The sample-containing dishes were weighed two times per day using a precision balance (ME204; Mettler-Toledo, Columbus, OH, USA) with an uncertainty of 0.0002 g until the weight loss or gain was lower than 0.001 g. The equilibrium moisture contents (X_{eq}) of the samples were determined according to AOAC method 934.06 (2000) with drying at 105°C for 24 hr using a convectional drying oven (HB-501M; Hanbaek Scientific Co.), and the values were reported as an average of triplicates. For comparison purpose, the moisture sorption isotherm of non-fermented sea tangle powder was also determined at 25°C.

2.6 | Modeling of moisture sorption isotherms

Moisture sorption isotherm data were fitted with eight types of empirical or semiempirical models (Table 2) to understand the sorption mechanism and predict X_{eq} at given a_w and temperature. The parameters of the models were obtained by nonlinear regression analysis using SPSS software (ver. 20.0; SPSS Inc., Chicago, IL, USA). The

TABLE 1 Water activities of saturated salt solutions at 4, 25, and 37°C (Greenspan, 1977)

Saturated salt solution	Temperature (°C)		
	4	25	37
Phosphorus pentoxide (P_4O_{10})	0.000	0.000	0.000
Lithium chloride (LiCl)	0.115	0.113	0.111
Potassium acetate (CH_3COOK)	0.235	0.225	0.204
Magnesium chloride ($MgCl_2$)	0.331	0.328	0.319
Potassium carbonate (K_2CO_3)	0.433	0.432	0.431
Magnesium nitrate ($Mg(NO_3)_2$)	0.590	0.529	0.488
Potassium iodide (KI)	0.735	0.689	0.674
Ammonium sulfate ($(NH_4)_2SO_4$)	0.804	0.802	0.797
Potassium nitrate (KNO_3)	0.960	0.936	0.919

TABLE 2 Models used to describe moisture sorption isotherms of probiotic-fermented sea tangle powder (Bejar, Mihoubi, & Kechaou, 2012; Iglesias, 2012; Maroulis et al., 1988)

Model	Mathematical expression
GAB	$X_{\text{eq}} = X_0 C K a_w / [(1 - K a_w) (1 - K a_w + C K a_w)]$
BET	$X_{\text{eq}} = X_0 C a_w / [(1 - a_w) (1 + (C - 1) a_w)]$
Henderson	$X_{\text{eq}} = [-\ln(1 - a_w/A)]^{1/B}$
Smith	$X_{\text{eq}} = A + (B \log(1 - a_w))$
Oswin	$X_{\text{eq}} = A (a_w / (1 - a_w))^B$
Halsey	$X_{\text{eq}} = [-A / (T \ln a_w)]^{1/B}$
Ferro-Fontan	$X_{\text{eq}} = [\gamma / \ln(\alpha/a_w)]^{1/r}$
Peleg	$X_{\text{eq}} = K_1 a_w^{n_1} + K_2 a_w^{n_2}$

Note: X_{eq} = equilibrium moisture content (g water/g dry matter); X_0 = monolayer moisture content (g water/g dry matter); a_w = water activity; T = absolute temperature (K); C , K , A , B , γ , α , r , K_1 , K_2 , n_1 , and n_2 are model parameters.

goodness of fit of each model was evaluated by calculating the coefficient of determination (R^2), the standard error (SE), and the mean relative percentage deviation modulus (M_r):

$$SE = \sqrt{\frac{\sum (Y_i - Y_{pi})^2}{df}} \quad (3)$$

$$M_r (\%) = \frac{100}{N} \sum_{i=1}^N \frac{|Y_i - Y_{pi}|}{Y_i} \quad (4)$$

where Y_i and Y_{pi} are experimental and predicted values of X_{eq} , respectively, df is the degree of freedom of regression model (N minus number of constants in model), and N is the population of experimental data. Residual plots of some models for the moisture sorption data were also determined. An R^2 value above 0.98 and the M_r value below 10% generally indicate a reasonable fit (Lomauro,

Bakshi, & Labuza, 1985). A model with a lower SE value and a residual value closer to zero is regarded more suitable.

2.7 | Determination of thermodynamic properties of moisture sorption

The enthalpy of sorption of water at a given X_{eq} (ΔH , J/mol) was determined by analyzing the moisture sorption isotherms obtained at different temperatures, using the modified form of the van't Hoff equation (Atkins & de Paula, 2006):

$$\left. \frac{\partial \ln(a_w)}{\partial (1/T)} \right|_{X_{eq}} = \frac{\Delta H}{R} \quad (5)$$

where a_w is the water activity, T is the absolute temperature (K), and R is universal gas constant (8.314 J/mol K). Assuming its temperature independence, the ΔH can be estimated from the slope of the regression line in the plot of $\ln a_w$ versus $1/T$ at a given X_{eq} .

The net isosteric heat of sorption of water a given X_{eq} (q_{st} , J/mol) is defined as $q_{st} = -\Delta H$, and the total isosteric heat of sorption of water at given X_{eq} and T (Q_{st} , J/mol) is given by:

$$Q_{st} = q_{st} + \lambda \quad (6)$$

where λ is the heat of vaporization of water at T (J/mol). The change of q_{st} with respect to X_{eq} is often described by an empirical exponential model (Tsami, 1991):

$$q_{st} = q_0 \exp(-X_{eq}/X_c) \quad (7)$$

where q_0 is the isosteric heat of sorption of monolayer water molecules (J/mol) and X_c is the characteristic moisture content (g water/g dry matter), at which $q_{st} = 0.37q_0$.

The Gibbs free energy (ΔG , J/mol) and entropy (ΔS , J/mol K) of sorption of water at a given X_{eq} are expressed as follows:

$$\Delta G = RT \ln a_w \quad (8)$$

$$\Delta S = \frac{\Delta H - \Delta G}{T} \quad (9)$$

Combining Equations (8) and (9) yields:

$$\ln a_w = \frac{\Delta H}{RT} - \frac{\Delta S}{R} \quad (10)$$

Equation (10) is an integrated form of Equation (5), assuming the temperature independence of ΔH and ΔS , and the ΔS value was estimated from the y-intercept of the regression line in the plot of $\ln a_w$ versus $1/T$ at a given X_{eq} .

The linearity between ΔH and ΔS was assessed to determine the mechanism of moisture sorption according to thermodynamic compensation theory (Krug, Hunter, & Grieger, 1976):

$$q_{st} = T_i \Delta S + \Delta G_i \quad (11)$$

where T_i (K) is the isokinetic temperature, at which all moisture sorption events in the series occur at the same rate, and ΔG_i is the free energy at T_i (J/mol). According to Krug et al. (1976), the thermodynamic compensation only exists when T_i is different from the harmonic mean temperature (T_h):

$$T_h = \frac{n}{\sum_{i=1}^n (1/T)} \quad (12)$$

where n is the number of moisture sorption isotherms. The moisture sorption is controlled by enthalpy when $T_i > T_h$, but by entropy when $T_i < T_h$.

3 | RESULTS AND DISCUSSION

3.1 | Proximate composition and particle size

The proximate analysis revealed that carbohydrates were the major component of both non-fermented (42.7%) and probiotic-fermented (65.7%) sea tangle powders (Table 3). The carbohydrate contents reported for other seaweed are 61.5% for *Ulva lactuca* flour, 58.4% for *Durvillaea antarctica* stem, and 70.9% for *D. antarctica* leaves (Ortiz et al., 2006). The moisture (3.2–8.1%), proteins (8.0–18.4%), lipids (0.0%), and ash (12.7–41.2%) contents of both sea tangle powders did not differ greatly from the values reported for other seaweed powders, such as *U. lactuca*, *D. antarctica*, and *Eucheuma denticulatum* (Ortiz et al., 2006; Portugal, Ladines, & Ardena, 1983; Wong & Cheung, 2000). The probiotic-fermented sea tangle powder showed higher protein and carbohydrate contents, but lower moisture and ash contents, compared to the non-fermented sea tangle powder (Table 3). This was attributed to the probiotic-fermented powder having a much lower salinity (5.2%) than the non-fermented powder (32.1%). The lipid contents of both sea tangle powders were almost negligible.

The $d_{4,3}$ of the probiotic-fermented powder (73.49 μm) was three times greater than that of non-fermented powder

TABLE 3 Proximate compositions of non-fermented and fermented sea tangle powders

Component (%)	Non-fermented	Fermented
Moisture	8.1 ± 0.2	3.2 ± 0.3
Proteins	8.0 ± 0.3	18.4 ± 0.2
Carbohydrates	42.7 ± 0.4	65.7 ± 0.4
Lipids	0.0 ± 0.0	0.0 ± 0.0
Ash	41.2 ± 0.3	12.7 ± 0.1

(23.96 μm). The span value of the probiotic-fermented sea tangle powder (1.82) was only half of that of the non-fermented sea tangle powder (3.45). These results indicate that the fermented sea tangle powder had more uniform and larger particles than the non-fermented sea tangle powder. During the fermentation, acid-induced protein aggregation could occur around the pI values of the proteins due to the production of lactic acid by *L. brevis*. In addition, the decrease in pH during fermentation would induce attractive interactions between proteins and anionic polysaccharides, such as the fucoidans in sea tangle, causing the formation of protein-polysaccharide complexes (Razzak, Kim, & Chung, 2016). Such acid-induced protein aggregation and protein-polysaccharide complexation during fermentation could be partly responsible for the more uniform and larger particles found in the fermented powder.

3.2 | Moisture sorption isotherms

The moisture sorption isotherms of *L. brevis*-fermented sea tangle powder at 4, 25, and 37°C are shown in Figure 1a. At all temperatures tested, the X_{eq} increased linearly as the a_w increased up to about 0.7, and then increased sharply with further increases in a_w . This is typical J-shaped type III moisture sorption behavior, which was also reported for several other brown and red algae, such as *F. vesiculosus* (Moreira, Chenlo, Sineiro, Arufe, et al., 2016), *B. bifurcate* (Moreira, Chenlo, Sineiro, Sánchez, et al., 2016), *K. alvarezii* (Senthil et al., 2011), *Gracilaria* (Lemus et al., 2008), and *Gelidium sesquipedale* (Mohamed et al., 2005). The high carbohydrate contents (42.71–65.74%) appear to primarily be responsible for the type III sorption behavior of the sea tangle powders (Brunauer, Deming, Deming, & Teller, 1940). Within the linear increase region ($a_w < 0.7$), the X_{eq} was

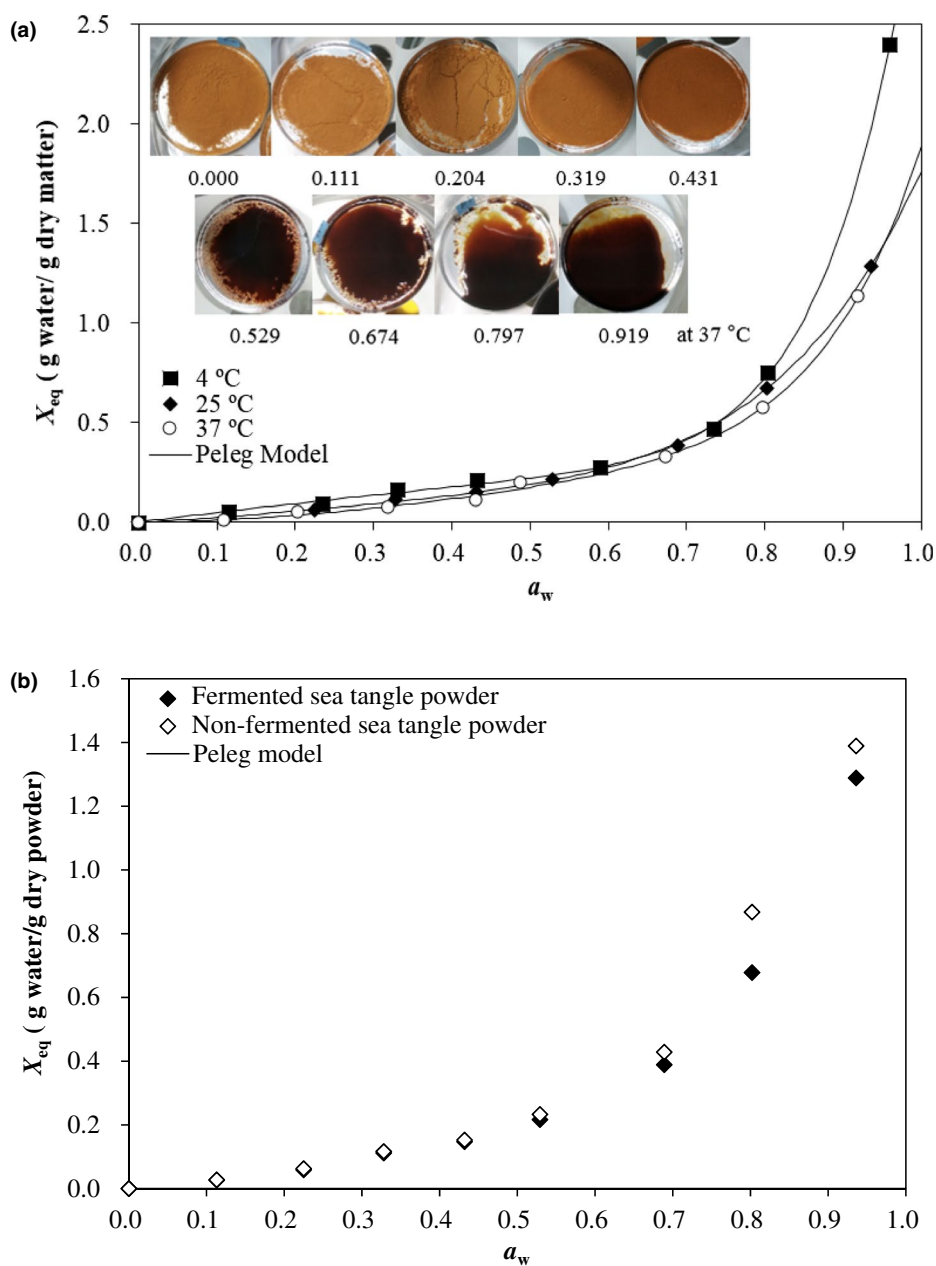


FIGURE 1 Moisture sorption isotherms of *L. brevis*-fermented sea tangle powder at 4, 25, and 37°C (a), and of non-fermented and *L. brevis*-fermented sea tangle powders at 25°C (b). Symbols represent experimental data and solid lines are simulated results obtained from the Peleg model

less than about 0.4 g water/g dry matter, but this value dramatically increased to 1.13 g water/g dry matter at 37°C, 1.29 g water/g dry matter at 25°C, and up to 2.40 g water/g dry matter at 4°C as the a_w further increased above 0.9 (Figure 1a). This moisture sorption capacity of the probiotic-fermented sea tangle powder was higher than that reported for other seaweeds, in which the X_{eq} was generally about 0.1–0.2 g water/g dry matter in the linear increase region (a_w values below about 0.6–0.7) and increased up to about 0.65–1.2 g water/g dry matter as the a_w increased further to about 0.9 (Lemus et al., 2008; Mohamed et al., 2005; Moreira, Chenlo, Sineiro, Arufe, et al., 2016; Moreira, Chenlo, Sineiro, Sánchez, et al., 2016; Senthil et al., 2011). Due to their high moisture sorption capacity, the sea tangle powders placed at $a_w > 0.5$ developed water bridges between the particles during the initial storage period, and were transformed to rubbery and even liquid states during storage, as shown in the pictures of Figure 1a.

The moisture sorption isotherm of probiotic-fermented sea tangle powder can be divided into three regions: (a) the low a_w region ($a_w < 0.2$), where water molecules are adsorbed on the surface of particles as a monolayer, (b) the intermediate a_w region ($0.2 < a_w < 0.7$), where water molecules are adsorbed as additional layers over the monolayer, and (c) the high a_w region ($a_w > 0.7$), where water molecules are condensed in the pores of the particles, followed by dissolution of soluble substances. As the particles are swollen due to the adsorption of water molecules, pores or void spaces may be newly created depending on the stability of the microstructure of the particles, in which more water molecules can be adsorbed and structurally entrapped (Kumar, Jha, Jain, Sahu, & Arora, 2012). A reason for the high moisture sorption capacity of probiotic-fermented sea tangle powder, especially in the high a_w region, is that the fermented sea tangle powder has a microstructure that is relatively unstable in response to water sorption compared to that of other reported fresh seaweeds; furthermore, its microstructure is altered, resulting in a more porous structure that can entrap a greater number of water molecules during the sorption process.

Smaller values of X_{eq} were measured at a higher temperature in the entire a_w range (Figure 1a); this was attributed to the higher temperature providing more kinetic energy to water molecules, which promoted the desorption of water molecules from their binding sites and thus resulted in a less hygroscopic powder (Palipane & Driscoll, 1993). A similar effect of temperature on moisture sorption was also reported for other brown and red algae, such as *B. bifurcate*, *Gracilaria*, and *G. sesquipedale*, at temperatures between approximately 5 and 55°C (Lemus et al., 2008; Mohamed et al., 2005; Moreira, Chenlo, Sineiro, Sánchez, et al., 2016). However, the opposite effect of temperature was reported for some dried fruits, such as raisin and date, which contain high amounts of sugar, but relatively low amounts of insoluble solids and proteins (Myhara & Sablani, 2001). This temperature effect on the isotherms was much greater at high a_w region, probably because the water molecules highly entrapped in the unstable porous microstructure formed at high a_w region were more easily desorbed by the increase in temperature.

Figure 1b shows that the non-fermented sea tangle powder had similar moisture sorption behavior to the probiotic-fermented sea

tangle powder at 25°C. The moisture sorption isotherm of non-fermented sea tangle powder was almost the same as that of probiotic-fermented sea tangle powder when $a_w < 0.7$, while slightly higher X_{eq} values were obtained for the non-fermented powder when $a_w > 0.7$. Because the $d_{4,3}$ of non-fermented sea tangle powder (23.96 μm) was only one-third that of probiotic-fermented sea tangle powder (73.49 μm), the higher moisture sorption of non-fermented powder is likely due to its smaller particle size and the resulting greater surface area for water adsorption. Additionally, the higher salinity content of the non-fermented sea tangle powder (32.14%) compared to the probiotic-fermented sea tangle powder (5.23%) may also contribute to the higher moisture sorption of the non-fermented powder.

3.3 | Modeling sorption isotherms

The parameters of eight isotherm models, estimated from the moisture sorption isotherm data of probiotic-fermented sea tangle powder, are summarized in Table 4. Considering the M_r , SE , and R^2 , the Peleg model had the best fit ($3.56\% \leq M_r \leq 11.92\%$, $0.008 \leq SE \leq 0.021$, and $0.998 \leq R^2 \leq 0.999$), followed by the GAB model ($5.78\% \leq M_r \leq 13.29\%$, $0.014 \leq SE \leq 0.036$, and $0.997 \leq R^2 \leq 0.999$), while the Henderson model had the poorest fit ($90.39\% \leq M_r \leq 96.45\%$, $0.040 \leq SE \leq 0.108$, and $0.985 \leq R^2 \leq 0.993$). The M_r showed an increasing trend as the temperature increased, except in the Henderson and Smith models, indicating that the modeling of moisture sorption isotherms became less reliable as temperature increased. Figure 2 shows the residual plots of GAB and Peleg models for the moisture sorption data. In general, the residuals of the Peleg model were more uniformly scattered and closer to zero than those of the GAB model, indicating that the Peleg model is more suitable than the GAB model for describing the moisture sorption isotherm of the fermented sea tangle powder.

The two parameters of the Peleg model, K_1 and K_2 , represent the initial rate of, and capacity for, moisture sorption, respectively (Turhan, Sayar, & Gunasekaran, 2002). The K_1 decreased greatly from 2.895 to 0.379, as the temperature increased from 4 to 25°C, indicating that the initial moisture sorption rate increased with temperature; meanwhile, no increase in the initial sorption rate was observed when the temperature increased further to 37°C ($K_1 = 0.568$) (Table 4). The K_2 increased greatly from 0.410 to 1.385, as the temperature increased from 4 to 25°C (Table 4), indicating a decrease in moisture sorption capacity as the temperature increased (Figure 1a). However, no further increase in K_2 was observed as the temperature increased from 25 to 37°C (K_2 at 37°C = 1.320), as was expected based on the marginal decrease in sorption capacity observed in the moisture sorption isotherms (Figure 1a). Similar trends of decreasing K_1 and increasing K_2 with an increase in temperature were observed for the moisture sorption of hazelnut kernels and chickpea soaking (Lopez et al., 1995; Turhan et al., 2002), but there have been no such reports for seaweed powders. The non-fermented sea tangle powder had values of K_1 (0.157) and K_2 (1.635), similar to those of the fermented sea tangle powder ($K_1 = 0.379$ and $K_2 = 1.385$) at 25°C,

TABLE 4 Parameters of sorption isotherm models, coefficient of determination (R^2), standard error (SE), and mean relative percentage deviation modulus (M_r) estimated for moisture sorption isotherms of probiotic-fermented sea tangle powder

Model	Parameters	Temperature (°C)		
		4	25	37
GAB	X_0	0.176	0.443	0.243
	C	2.297	0.476	0.751
	K	0.968	0.837	0.904
	R^2	0.999	0.999	0.997
	SE	0.036	0.014	0.019
	M_r (%)	7.61	5.78	13.29
BET	X_0	0.099	0.089	0.098
	C	113.4	22.68	5.673
	R^2	0.981	0.943	0.978
	SE	0.118	0.116	0.063
	M_r (%)	22.29	25.69	25.55
Henderson	A	1.318	1.394	1.419
	B	0.306	0.452	0.420
	R^2	0.985	0.993	0.989
	SE	0.108	0.040	0.044
	M_r (%)	93.46	96.45	90.39
Smith	A	-0.180	-0.077	-0.082
	B	-0.715	-0.473	-0.447
	R^2	0.930	0.981	0.969
	SE	0.217	0.054	0.065
	M_r (%)	81.68	15.25	36.62
Oswin	A	0.247	0.228	0.187
	B	0.716	0.655	0.747
	R^2	0.998	0.986	0.993
	SE	0.040	0.056	0.036
	M_r (%)	7.62	19.59	20.17
Halsey	A	24.40	28.66	31.06
	B	1.264	1.329	1.152
	R^2	0.995	0.971	0.982
	SE	0.257	0.078	0.055
	M_r (%)	24.14	25.29	26.17
Ferro-Fontan	Γ	0.211	0.444	0.342
	A	1.062	1.383	1.265
	R	0.839	0.503	0.553
	R^2	0.998	0.999	0.998
	SE	0.032	0.012	0.021
	M_r (%)	8.95	4.81	13.56
Peleg	K_1	2.895	0.379	0.568
	K_2	0.410	1.385	1.320
	n_1	9.014	1.188	1.731
	n_2	0.923	5.874	8.519
	R^2	0.999	0.999	0.998
	SE	0.016	0.008	0.021
	M_r (%)	5.31	3.56	11.92

as was expected based on their similar moisture sorption isotherms (Figure 1b).

The three parameters in the GAB model are as follows: X_0 , the monolayer moisture content (g water/g dry matter), which represents the availability of sorption sites; C, which is related to the binding strength between the monolayer water molecules and the surface sorption sites; and K, which is a correction factor for water molecules in the multilayer relative to the bulk water (Sormoli & Langrish, 2015). The X_0 was estimated to be 0.176, 0.443, and 0.243 g water/g dry matter at 4, 25, and 37°C, respectively (Table 4), and indicating the temperature independence of X_0 , where the bivariate correlations analysis performed between the temperature and X_0 using the SPSS software showed a p -value of 0.348. Gabas, Telis, Sobral, and Telis-Romero. (2007) also reported temperature independence of the X_0 value for pineapple pulp powder, while some studies reported that the X_0 decreased as the temperature increased due to the increased kinetic energy of bound water at a higher temperature, resulting in greater water desorption (Palipane & Driscoll, 1993; Sormoli & Langrish, 2015). The temperature independence of X_0 could be attributed to the water-induced collapse of the microstructure of the probiotic-fermented sea tangle powder with high carbohydrate and protein contents (84.12%) during the sorption process, especially at the high a_w region, as discussed in moisture sorption isotherms. The X_0 values obtained from the GAB model were higher than those estimated using the BET model (0.089–0.099 g water/g dry matter) (Table 4). This is because the BET model takes only the monolayer moisture sorption on the powder surface into account, while the GAB model addresses the high moisture sorption capacity of the probiotic-fermented sea tangle powder through swelling, water-induced microstructure collapse, and the resulting creation of new sorption sites (Kaderides & Goula, 2017). The C value was much higher at 4°C compared to those obtained at higher temperatures (Table 4). This indicates that binding between the monolayer water molecules and sorption sites on the powder surface was favored at a lower temperature, probably due to the stronger hydrogen bonding and lower kinetic energy of water molecules at a lower temperature. The K value was in the range between 0.837 and 0.968 (Table 4). The closer the value of K is to 1, the smaller the difference between the properties of multilayer water and pure water, such that the heat of sorption of multilayer water becomes the same as the heat of condensation of pure water when $K = 1$ (Sormoli & Langrish, 2015).

3.4 | Thermodynamic properties

Figure 3 shows that the q_{st} for the probiotic-fermented sea tangle powder sharply decreased from 15.02 to 3.59 kJ/mol, as the X_{eq} increased from 0.02 to 0.21 g water/g dry matter, followed by a gradual decrease to 0.49 kJ/mol as the X_{eq} increased further to 1.29 g water/g dry matter at 4–37°C. At the beginning of moisture sorption in the low X_e region, the water molecules were tightly bound to the sorption sites on the surface of the powder, forming a monolayer with high interaction energy. As the moisture sorption progressed in the intermediate X_e region, the interaction energy between water and the powder became weaker; thus, it became easier to remove

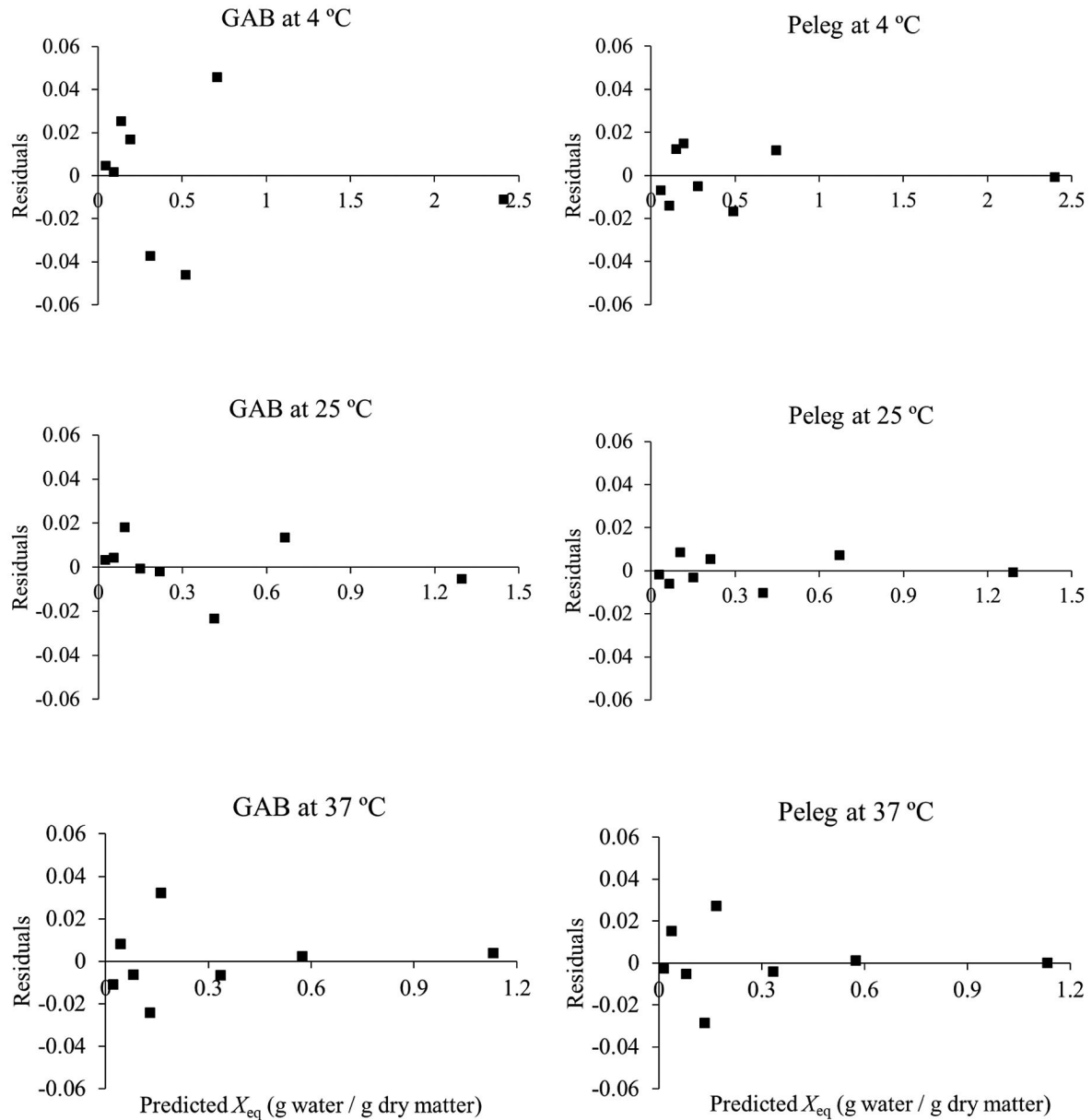


FIGURE 2 Plots of residuals fit of GAB and Peleg models to the moisture sorption data of *L. brevis*-fermented sea tangle powder at 4, 25, and 37°C

water molecules from the powder. When a sufficiently large amount of water was adsorbed on the powder in the high X_e region, the interaction energy became close to that between pure water molecules, that is, the heat of vaporization of water. The decrease in q_{st} with respect to X_{eq} was adequately described ($R^2 = 0.991$) by the Tsami model (Equation 7); the two model parameters, that is, the q_0 and the X_c at which $q_{st} = 0.37q_0$, were determined to be 18.19 kJ/mol and 0.12 g water/g dry matter, respectively. Moreira, Chenlo, Sineiro, Arufe, et al. (2016) reported that the q_{st} of *F. vesiculosus* (a brown alga) decreased from 21.24 to 0.01 kJ/mol as the X_{eq} increased from 0.07 to 0.34 g water/g dry matter. Moreira, Chenlo, Sineiro, Sánchez, et al. (2016) also reported a decrease in the q_{st} value of *B. bifurcate* (a brown alga), from 18.67 to 0.04 kJ/mol, as the X_{eq} increased from 0.05 to 0.17 g water/g dry matter. The q_{st} of the probiotic-fermented

sea tangle powder decreased much more slowly as the X_{eq} increased, in comparison to the q_{st} values reported for the other two brown algae. The relatively higher interaction energy between water and the fermented sea tangle powder, especially at high moisture levels, may explain why the fermented sea tangle powder had a much higher moisture sorption capacity than that reported for the other two brown algae, as mentioned in moisture sorption isotherms.

Figure 4a shows that both the ΔG and ΔS of moisture sorption for the probiotic-fermented sea tangle powder were negative in the entire range of X_{eq} values examined, and exhibited sharp increases at low X_{eq} (<0.38) followed by a gradual approach to zero as the X_{eq} further increased. The negative ΔS indicates that the moisture sorption of the probiotic-fermented sea tangle powder was entropically unfavorable; water molecules lost their degrees

FIGURE 3 Net isosteric heat of sorption (q_{st}) and moisture sorption isotherm at 25°C for *L. brevis*-fermented sea tangle powder. Symbols represent experimental data, and solid and dotted lines are the moisture sorption isotherm simulated by the Peleg model and q_{st} simulated by the Tsami model (Equation 7), respectively

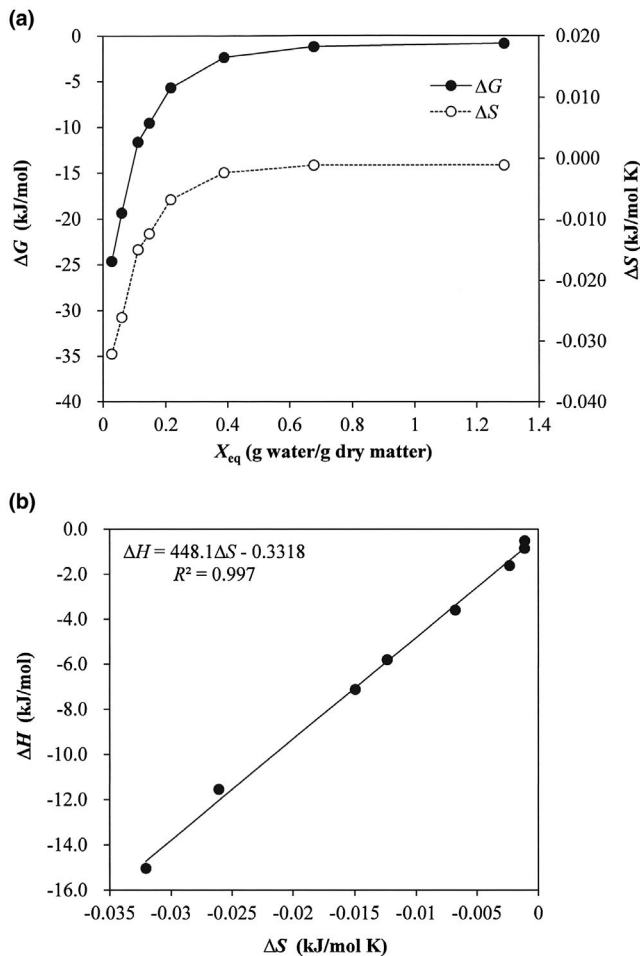
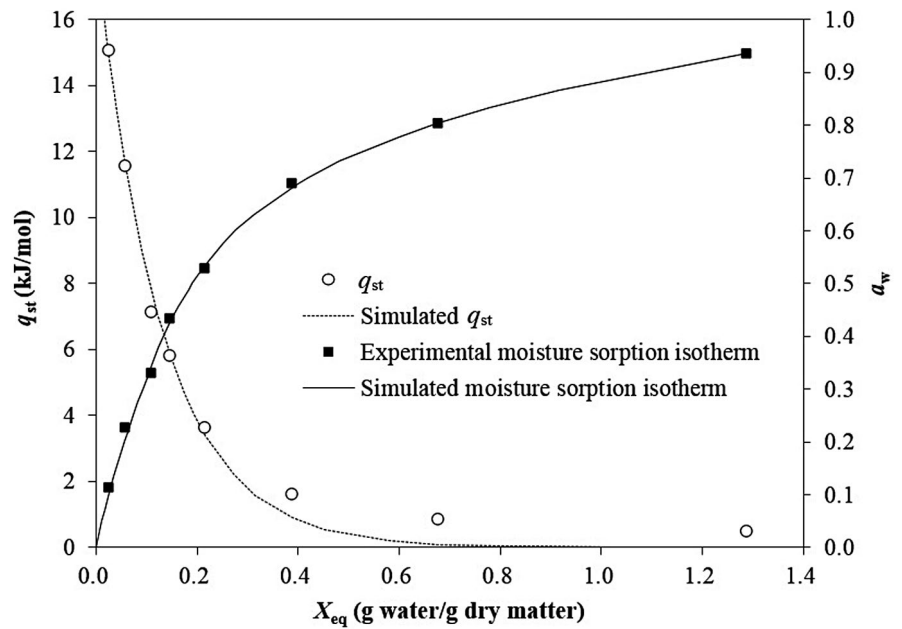


FIGURE 4 Changes in Gibbs free energy (ΔG) and entropy (ΔS) of moisture sorption with respect to the equilibrium moisture content (X_{eq}) for *L. brevis*-fermented sea tangle powder (a), and linearity between enthalpy (ΔH) and entropy (ΔS) of moisture sorption (b)

of freedom by adsorbing to the sorption sites. The increase in ΔS to zero as the X_{eq} increased is due to the decrease in the number of available sorption sites as sorption progressed. Despite the negative ΔS , the ΔG was negative due to the highly negative $\Delta H (= -q_{st})$, indicating that the moisture sorption process was spontaneous. The approach of ΔG to zero as the X_{eq} increased indicates that the moisture sorption was more favorable at lower X_{eq} . The negative ΔH indicates that the moisture sorption of the fermented sea tangle powder was an exothermic, energetically favorable process. The approach of ΔH to zero as the X_{eq} increased was due to the decrease in the interaction energy between water and the powder, which also explained the decrease in q_{st} as the X_{eq} increased (as discussed above).

A linear correlation ($R^2 = 0.997$) was found between ΔH and ΔS (Figure 4b). Therefore, the T_p at which all moisture sorption events in the series occur at the same rate, and the ΔG at T_i (ΔG_i) were obtained for the fermented sea tangle powder using Equation (11): $T_i = 448.1$ K (174.8°C) and $\Delta G_i = -0.3318$ kJ/mol. This T_i was slightly higher than that reported for *B. bifurcate* (404.4 K), which is a brown alga (Moreira, Chenlo, Sineiro, Sánchez, et al., 2016); however, it is much higher than the T_i reported for another brown alga, *F. Vesiculosus* (363.2 K; Moreira, Chenlo, Sineiro, Arufe, et al., 2016). The T_h obtained from Equation (11) was 294.5 K (21.4°C), which was significantly lower than the T_p . This indicates that the enthalpy–entropy compensation existed for the moisture sorption of the probiotic-fermented sea tangle powder, and that the moisture sorption was an enthalpy-driven process under the conditions examined, as also mentioned above. The moisture sorption of the two brown algae, *B. bifurcate* and *F. Vesiculosus*, was also reported to be controlled by enthalpy (Moreira, Chenlo, Sineiro, Arufe, et al., 2016; Moreira, Chenlo, Sineiro, Sánchez, et al., 2016). The negative ΔG_i suggests that the fermented sea tangle powder favors moisture adsorption rather than desorption even at T_p .

4 | CONCLUSIONS

The present study demonstrated that the *L. brevis*-fermented sea tangle powder had typical J-shaped type III moisture sorption behavior at 4, 25, and 37°C. The X_{eq} increased linearly as the a_w increased to about 0.7, but remained below about 0.4 g water/g dry matter, followed by a sharp increase up to 2.40 g water/g dry matter at 4°C with a further increase in a_w to above 0.9. Due to high moisture sorption, the sea tangle powders stored at $a_w > 0.5$ were found to be transformed to rubbery or liquid states during storage. This high moisture sorption capacity of the fermented sea tangle powder, especially at high a_w levels, as compared to the capacities reported for other seaweeds, may be attributed to its microstructure being relatively unstable to moisture sorption, and thus altered to a more porous structure that can entrap more water molecules during the sorption process. The sea tangle powder was less hygroscopic at a higher temperature in the entire range of a_w , because water molecules became more kinetically active and more easily desorbed from their binding sites at a higher temperature. The Peleg and GAB models were found to most accurately describe the moisture sorption isotherms among eight sorption models. The Peleg model showed that, in general, a higher resulted in a faster initial moisture sorption rate, but a smaller moisture sorption capacity. The GAB model yielded monolayer moisture contents of 0.176, 0.443, and 0.243 g water/g dry matter at 4, 25, and 37°C, respectively. The temperature independence of monolayer moisture content is probably due to the water-induced collapse of the microstructure of the sea tangle powder, which contains high carbohydrate and protein contents (84.12%). The GAB model suggested that the binding between the monolayer water molecules and the powder sorption sites was favored at a lower temperature, probably due to the stronger hydrogen bonding and lower kinetic energy of the water molecules. The q_{st} showed an exponential decrease as the X_{eq} increased, as also reported for other seaweeds, showing that the interaction energy between water and the powder was strong in the monolayer, became weaker as the moisture sorption progressed due to the multilayer adsorption, and became close to the heat of vaporization of pure water when a sufficient amount of water was adsorbed. The analyses on ΔH , ΔS , and ΔG showed that the moisture sorption of the sea tangle powder was an entropically unfavorable, exothermic, enthalpy-driven spontaneous process under the conditions examined, and was more favored at lower X_{eq} values, as also reported for other seaweeds. The enthalpy-entropy compensation existed with a T_i of 448.1 K. The present study provides information essential for understanding the strongly hygroscopic nature, and resulting low storage stability, of the commercially available *L. brevis*-fermented sea tangle powder, which currently limits its easy and convenient handling and application.

ACKNOWLEDGMENTS

This research was part of a project titled "Development of Global Senior-friendly Healthy Functional Food Materials from Marine Resources" funded by the Ministry of Oceans and Fisheries, Korea.

CONFLICT OF INTEREST

The authors have declared no conflicts of interest for this article.

ORCID

Daeung Yu  <https://orcid.org/0000-0002-2185-4959>

REFERENCES

- AOAC. (2000). *Official methods of analysis of AOAC international* (17th ed.). Rockville, MD: AOAC International.
- Atkins, P., & de Paula, J. (2006). *Physical chemistry* (8th ed.). Oxford, UK: Oxford University Press.
- Bejar, A. K., Mihoubi, N. B., & Kechaou, N. (2012). Moisture sorption isotherms-experimental and mathematical investigations of orange (*Citrus sinensis*) peel and leaves. *Food Chemistry*, 132, 1728–1735. <https://doi.org/10.1016/j.foodchem.2011.06.059>
- Brunauer, S., Deming, L. S., Deming, W. E., & Teller, E. (1940). On a theory of the van der Waals adsorption of gases. *Journal of the American Chemical Society*, 62, 1723–1732. <https://doi.org/10.1021/ja01864a025>
- Gabas, A. L., Telis, V. R. N., Sobral, P. J. A., & Telis-Romero, J. (2007). Effect of maltodextrin and arabic gum in water vapor sorption thermodynamic properties of vacuum dried pineapple pulp powder. *Journal of Food Engineering*, 82, 246–252. <https://doi.org/10.1016/j.jfoodeng.2007.02.029>
- Greenspan, L. (1977). Humidity fixed points of binary saturated aqueous solutions. *Journal of Research of the National Bureau of Standards*, 81, 89–96. <https://doi.org/10.6028/jres.081A.011>
- Haroun-Bouhedja, F., Ellouali, M., Sinquin, C., & Boisson-Vidal, C. (2000). Relationship between sulfate groups and biological activities of fu-cans. *Thrombosis Research*, 100, 453–459. [https://doi.org/10.1016/S0049-3848\(00\)00338-8](https://doi.org/10.1016/S0049-3848(00)00338-8)
- Iglesias, H. (2012). *Handbook of food isotherms: Water sorption parameters for food and food components*. New York, NY: Elsevier.
- Kaderides, K., & Goula, A. M. (2017). Development and characterization of a new encapsulating agent from orange juice by-products. *Food Research International*, 100, 612–622. <https://doi.org/10.1016/j.foodres.2017.07.057>
- Kang, Y. M., Lee, B. J., Kim, J. I., Nam, B. H., Cha, J. Y., Kim, Y. M., ... Je, J. Y. (2012). Antioxidant effects of fermented sea tangle (*Laminaria japonica*) by *Lactobacillus brevis* BJ20 in individuals with high level of γ -GT: A randomized, double-blind, and placebo-controlled clinical study. *Food and Chemical Toxicology*, 50, 1166–1169. <https://doi.org/10.1016/j.fct.2011.11.026>
- Kang, Y. M., Qian, Z. J., Lee, B. J., & Kim, Y. M. (2011). Protective effect of GABA-enriched fermented sea tangle against ethanol-induced cytotoxicity in HepG2 cells. *Biotechnology and Bioprocess Engineering*, 16, 966–970. <https://doi.org/10.1007/s12257-011-0154-z>
- Keup, L., & Bayless, J. (1964). Fish distribution at varying salinities in Neuse River basin, North Carolina. *Chesapeake Science*, 5, 119–123. <https://doi.org/10.2307/1351370>
- Krug, R. R., Hunter, W. G., & Grieger, R. A. (1976). Enthalpy-entropy compensation. 1. Some fundamental statistical problems associated with the analysis of van't Hoff and Arrhenius data. *The Journal of Physical Chemistry*, 80, 2335–2341. <https://doi.org/10.1021/j100562a006>
- Kumar, A., Jha, A., Jain, P., Sahu, J. K., & Arora, S. (2012). Moisture sorption characteristics of *lal peda* at different storage temperatures. *Food Research International*, 49, 373–378. <https://doi.org/10.1016/j.foodres.2012.07.050>

- Lee, B. J., Kim, J. S., Kang, Y. M., Lim, J. H., Kim, Y. M., Lee, M. S., ... Je, J. Y. (2010). Antioxidant activity and γ -aminobutyric acid (GABA) content in sea tangle fermented by *Lactobacillus brevis* BJ20 isolated from traditional fermented foods. *Food Chemistry*, 122, 271–276. <https://doi.org/10.1016/j.foodchem.2010.02.071>
- Lemus, R. A., Pérez, M., Andrés, A., Roco, T., Tello, C. M., & Vega, A. (2008). Kinetic study of dehydration and desorption isotherms of red alga *Gracilaria*. *LWT-Food Science and Technology*, 41, 1592–1599. <https://doi.org/10.1016/j.lwt.2007.10.011>
- Lomauro, C. J., Bakshi, A. S., & Labuza, T. P. (1985). Evaluation of food moisture sorption isotherm equations. Part I. Fruit, vegetable and meat products. *Lebensmittel-Wissenschaft und Technologie*, 18, 111–117. <https://doi.org/10.4172/2157-7110.1000319>
- Lopez, A., Pique, M. T., Clop, M., Tacias, J., Romero, A., Boatella, J., & Garcia, J. (1995). The hygroscopic behaviour of the hazelnut. *Journal of Food Engineering*, 25, 197–208. [https://doi.org/10.1016/0260-8774\(94\)00021-Z](https://doi.org/10.1016/0260-8774(94)00021-Z)
- Marine Bioprocess. (2018, August 10). Retrieved from http://www.mbpcc.co.kr/03_01.asp/
- Maroulis, Z. B., Tsami, E., Marinou-Kouris, D., & Saravacos, G. D. (1988). Application of the GAB model to the moisture sorption isotherms for dried fruits. *Journal of Food Engineering*, 7, 63–78. [https://doi.org/10.1016/0260-8774\(88\)90069-6](https://doi.org/10.1016/0260-8774(88)90069-6)
- Mohamed, L. A., Kouhila, M., Lahsasni, S., Jamali, A., Idlimam, A., Rhazi, M., ... Mahrouz, M. (2005). Equilibrium moisture content and heat of sorption of *Gelidium sesquipedale*. *Journal of Stored Products Research*, 41, 199–209. <https://doi.org/10.1016/j.jspr.2004.03.001>
- Moreira, R., Chenlo, F., Sineiro, J., Arufe, S., & Sexto, S. (2016). Drying temperature effect on powder physical properties and aqueous extract characteristics of *Fucus vesiculosus*. *Journal of Applied Phycology*, 28, 2485–2494. <https://doi.org/10.1007/s10811-015-0744-9>
- Moreira, R., Chenlo, F., Sineiro, J., Sánchez, M., & Arufe, S. (2016). Water sorption isotherms and air drying kinetics modelling of the brown seaweed *Bifurcaria bifurcata*. *Journal of Applied Phycology*, 28, 609–618. <https://doi.org/10.1007/s10811-015-0553-1>
- Myhara, R. M., & Sablani, S. (2001). Unification of fruit water sorption isotherms using artificial neural networks. *Drying Technology*, 19, 1543–1554. <https://doi.org/10.1081/DRT-100107258>
- Ortiz, J., Romero, N., Robert, P., Araya, J., Lopez-Hernández, J., Bozzo, C., ... Rios, A. (2006). Dietary fiber, amino acid, fatty acid and tocopherol contents of the edible seaweeds *Ulva lactuca* and *Durvillaea antarctica*. *Food Chemistry*, 99, 98–104. <https://doi.org/10.1016/j.foodchem.2005.07.027>
- Palipane, K. B., & Driscoll, R. H. (1993). Moisture sorption characteristics of in-shell macadamia nuts. *Journal of Food Engineering*, 18, 63–76. [https://doi.org/10.1016/0260-8774\(93\)90075-U](https://doi.org/10.1016/0260-8774(93)90075-U)
- Portugal, T. R., Ladines, E. O., & Ardena, S. S. (1983). Nutritive value of some Philippine seaweeds, part 2: Proximate amino acid and vitamin composition. *Philippine Journal of Nutrition*, 78, 166–172.
- Razzak, M. A., Kim, M., & Chung, D. (2016). Elucidation of aqueous interactions between fish gelatin and sodium alginate. *Carbohydrate Polymers*, 148, 181–188. <https://doi.org/10.1016/j.carbpol.2016.04.035>
- Senthil, A., Mamatha, B. S., Vishwanath, P., Bhat, K. K., & Ravishankar, G. A. (2011). Studies on development and storage stability of instant spice adjunct mix from seaweed (*Euclima*). *Journal of Food Science and Technology*, 48, 712–717. <https://doi.org/10.1007/s13197-010-0165-3>
- Sormoli, M. E., & Langrish, T. A. (2015). Moisture sorption isotherms and net isosteric heat of sorption for spray-dried pure orange juice powder. *LWT-Food Science and Technology*, 62, 875–882. <https://doi.org/10.1016/j.lwt.2014.09.064>
- Tsami, E. (1991). Net isosteric heat of sorption in dried fruits. *Journal of Food Engineering*, 14, 327–335. [https://doi.org/10.1016/0260-8774\(91\)90022-K](https://doi.org/10.1016/0260-8774(91)90022-K)
- Turhan, M., Sayar, S., & Gunasekaran, S. (2002). Application of Peleg model to study water absorption in chickpea during soaking. *Journal of Food Engineering*, 53, 153–159. [https://doi.org/10.1016/S0260-8774\(01\)00152-2](https://doi.org/10.1016/S0260-8774(01)00152-2)
- Wang, J., Zhang, Q., Zhang, Z., & Li, Z. (2008). Antioxidant activity of sulfated polysaccharide fractions extracted from *Laminaria japonica*. *International Journal of Biological Macromolecules*, 42, 127–132. <https://doi.org/10.1016/j.ijbiomac.2007.10.003>
- Wong, K. H., & Cheung, P. C. (2000). Nutritional evaluation of some subtropical red and green seaweeds: Part I—Proximate composition, amino acid profiles and some physico-chemical properties. *Food Chemistry*, 71, 475–482. [https://doi.org/10.1016/S0308-8146\(00\)00175-8](https://doi.org/10.1016/S0308-8146(00)00175-8)
- Yuan, Y. V., & Walsh, N. A. (2006). Antioxidant and antiproliferative activities of extracts from a variety of edible seaweeds. *Food and Chemical Toxicology*, 44, 1144–1150. <https://doi.org/10.1016/j.fct.2006.02.002>

How to cite this article: Yu D, Kwon G, Kim M, et al. Moisture sorption characteristics of probiotic-fermented sea tangle powder and its thermodynamic properties. *J Food Process Preserv*. 2019;43:e13991. <https://doi.org/10.1111/jfpp.13991>